NJC

Accepted Manuscript

This is an *Accepted Manuscript*, which has been through the Royal Society of Chemistry peer review process and has been accepted for publication.

Accepted Manuscripts are published online shortly after acceptance, before technical editing, formatting and proof reading. Using this free service, authors can make their results available to the community, in citable form, before we publish the edited article. We will replace this *Accepted Manuscript* with the edited and formatted *Advance Article* as soon as it is available.

You can find more information about *Accepted Manuscripts* in the Information for Authors.

Please note that technical editing may introduce minor changes to the text and/or graphics, which may alter content. The journal's standard Terms & Conditions and the Ethical guidelines still apply. In no event shall the Royal Society of Chemistry be held responsible for any errors or omissions in this *Accepted Manuscript* or any consequences arising from the use of any information it contains.

ROYAL SOCIETY OF CHEMISTRY

www.rsc.org/njc

NJC

RSC Publishing

ARTICLE

Synthesis of Perovskite-type Manganites $Yb_{1-x}Dy_xMnO_3$（$0.1\leq x\leq 0.5$）*via* Solid-State Reaction and High-pressure Flux Method Followed by Structural Characterization and Magnetic Property Studies

Cite this: DOI: 10.1039/x0xx00000x

Received ooth January 2012,
Accepted ooth January 2012

DOI: 10.1039/x0xx00000x

www.rsc.org/

Yingnan Zhang, [a] Fuyang Liu, [a] Tong Zheng, [a] Ziqing Zhang, [a] Wei Liu, [a] Xudong Zhao [a,*], Xiaoyang Liu [a,*]

A series of hexagonal perovskite-type compounds $Yb_{1-x}Dy_xMnO_3$ ($0.1\leq x\leq 0.5$) have been prepared by the traditional solid-state reaction method at 1573 K, and a single crystal orthorhombic perovskite-type compound $Yb_{0.5}Dy_{0.5}MnO_3$ has been also obtained by a high-pressure flux method at 1273 K under 5 GPa high pressure. Final products are fully characterized by XRD and XPS analyses, and then subject to magnetic measurements. It appears that the hexagonal $Yb_{1-x}Dy_xMnO_3$ ($0.1\leq x\leq 0.5$) compounds have shown antiferromagnetic property with a Néel temperature of 10 K, and canted antiferromagnetic behaviour is clearly evident at a lower temperature. Plus, it is found that the magnetization of $Yb_{1-x}Dy_xMnO_3$ increases with the rise of Dy content. The orthorhombic $Yb_{0.5}Dy_{0.5}MnO_3$ single crystal has been found to be paramagnetic, differ from $RMnO_3$ reported in the literature, which is antiferromagnetic due to subtle structural difference.

Introduction

Multiferroics are promising materials for the development of next-generation memory devices, mostly because their magnetic moments can be controlled electrically with fairly low power consumption. Perovskite-type oxides like ABO_3, are the most abundant minerals on earth, and they seem to be involved in multiple important functions such as ferroelectricity and magnetism.[1-4] Even though ferroelectric and magnetic orders tend to exclude each other, they can coexist in specific occasions like manganite perovskites. For rare earth manganites $RMnO_3$, when the ionic radius of R(R=Ho, Er, Tm, Yb, Lu, and Y) is small, they crystallize in a hexagonal structure; however, when the ionic radius R (R=La, Ce, Pr, Nd, Sm, Eu, Gd, Tb, and Dy) is large, they crystallize in an orthorhombic structure. Particularly, such materials have been found to be of multi-ferroic properties as well as strong coupling between electric and magnetic dipoles,[5-8] thus, studies have been carried out intensively by many groups, affording several classes of manganite compounds. In general, multi-ferroic materials can be classified into two types: type I, in which magnetism and ferroelectricity coexist in an independent manner; type II, in which magnetism and ferroelectricity coexist, but the later is originated from the former.[9] Specifically, hexagonal $YbMnO_3$ and the orthorhombic $DyMnO_3$ are the most representative compounds for type I and type II multi-ferroic materials, respectively.[10]

Recently, doped perovskite manganites have received much attention due to their tunable electronic and magnetic properties. On one hand, extensive investigations have been carried out on the $RE_{1-x}R_xMnO_3$ (RE = rare earth ion, R = alkaline earth ion), in which efforts have been focused on understanding how transporting and magnetic properties can be influenced by the size of cations as well as the disorder effect at the A-site. Such impacts, would certainly change the valence state of Mn ions and produce holes in the *d* band, ultimately resulting in colossal magnetoresistence effect, i.e. a large decrease to the electric resistivity accompanied by a transition from paramagnetic to ferromagnetic. On the other hand, the disorder effect of $RA_xMn_{1-x}O_3$ (A is Fe or Cr) system has been explored at the B-site, such as in compound Y_2FeMnO_6.[11] Notably, it appears that the magnetic exchange interaction has changed from the original Mn^{3+}-O^{2-}-Mn^{3+} antiferromagnetic super-exchange interaction to the ultra Fe^{3+}-O^{2-}-Mn^{3+} antiferromagnetic super-exchange interaction, which finally evolves to the Fe^{3+}-O^{2-}-Fe^{3+} super antiferromagnetic exchange interaction. Nevertheless, doping at B-site of manganites seems to have detrimental effect on their magnetic properties, thus ferroelectricity and ferromagnetism can no longer co-exist. So far, researches of manganite doping are mostly centered on type I multi-ferroics, and reports on type II multi-ferroics are fairly rare, especially for compounds doped with different rare earth metals at the A-site which presumably could modulate magnetic properties and alleviate the influences from structural changes. For instance, type I multiferroic material, $YbMnO_3$ can be modified to its type II counterpart by substituting to Tb element at the A-site, and its magnetic properties turned out to change gradually with doping.[12]

Generally, $RMnO_3$ compounds are synthesized by traditional solid-state reactions, or hydrothermal methods under mild conditions.

Specifically, approaches such as fusion method, floating zone melting method atmospheric flux method have been employed to produce single-crystal rare earth manganites, there are many methods.[13-15] In addition, it has been found that the crystal structure can be altered under high pressure conditions without doping, which provides a viable approach to exploring the influence of structural change on magnetic properties. As a matter of fact, high-pressure flux method has been proven to be one of the most successful methods for the high-pressure synthesis of single-crystal transition metals,[16] such as lanthanide elements[17] and uranium-based silicates.[18,19] To the best of our knowledge, the preparation of single crystal rare earth manganites under high pressure conditions has not been reported so far.

Hexagonal $YbMnO_3$ and orthorhombic $DyMnO_3$ are the most representative compounds for type I and type II multiferroic materials. In this work, we envision that doping Dy element into the $YbMnO_3$ crystal structure would produce novel materials featuring excellent properties. Indeed, a series of *h*-$Yb_{1-x}Dy_xMnO_3$ ($0.1\leq x\leq 0.5$) compounds has been readily prepared and subject to comprehensive spectral characterizations. Particularly, single crystal manganite *o*-$Yb_{0.5}Dy_{0.5}MnO_3$ has been synthesized by either traditional solid-state reaction method or high pressure flux method. Finally, the molecular structure and magnetic properties of manganites obtained have been thoroughly investigated.

Experimental Section

Synthesis of $Yb_{1-x}Dy_xMnO_3$ ($0.1\leq x\leq 0.5$)

The hexagonal $Yb_{1-x}Dy_xMnO_3$ ($0.1\leq x\leq 0.5$) compounds were prepared by the traditional solid-state reaction method. Mn_2O_3, Yb_2O_3, and Dy_2O_3 were obtained from Alfa Aesar and then used as received. At first, stoichiometric amounts of starting materials were mixed and grounded to produce a homogeneous mixture, which was then pressed and sintered at 1573 K for 20 h under ambient pressure. It is known that Mn_2O_3 can decompose at 1213 K to generate Mn_3O_4 and oxygen, thus the actual reacting species in this synthesis should be Mn_3O_4.

At this point, the resulting $Yb_{0.5}Dy_{0.5}MnO_3$ material after sintering was used as the starting materials for next steps. The orthorhombic $Yb_{0.5}Dy_{0.5}MnO_3$ single crystal has been prepared with flux method under high pressure and high temperature conditions in a Walker-type high-pressure apparatus. The mass ratio of $Yb_{0.5}Dy_{0.5}MnO_3$ to KCl flux was 3:1. Subsequently, the mixture after pressing was placed in a platinum capsule, which was then subjected to a 5 GPa pressure at 1273 K for 2 hours. Finally, the temperature was first allowed to decrease from 1273 K to 1073 K within one hour, and then quenched to room temperature before releasing pressure. Samples obtained were washed with distilled water to remove KCl residues.

Characterization of $Yb_{1-x}Dy_xMnO_3$ ($0.1\leq x\leq 0.5$)

The X-ray diffraction (XRD) patterns of sample powders had been determined at room temperature using a Rigaku D/Max 2550 X-ray diffractometer with Cu *Ka* radiation at 50 kV and 200 mA. (λ= 0.71073 Å). The X-ray powder diffraction (XRD) spectra of single crystals were collected on Bruker D8 Discover diffractometer. All diffraction data were collected within the range of $10°\leq 2\theta \leq 120°$ at the step rate of 0.02°. The valence states of samples were determined by X-ray photoelectron spectroscopy (XPS, ESCALAB250, USA) analysis. Magnetism was measured on a superconducting quantum interference device (SQUID, Quantum Design Inc.) with a magnetometer between 5 and 300 K and a measuring field of H = 50 Oe in zero-field cooled (ZFC) and field-cooling (FC) mode. Magnetic hysteresis loops *M(H)* were measured at 5 K and 20 K.

Results and Discussion

The doped perovskite manganites, $Yb_{1-x}Dy_xMnO_3$ ($0.1\leq x\leq 0.5$), with the tunable electronic and magnetic properties were prepared by the traditional solid-state reaction method at 1573 K. The XRD patterns of hexagonal $Yb_{1-x}Dy_xMnO_3$ ($0.1\leq x\leq 0.5$) manganites were shown in Fig. 1. It appeared that all compounds were pure phase and they crystallize in the hexagonal perovskite structure with a space group of $P6_3cm$.[20] The XRD pattern between 15 and 35° was shown in the inset of Fig. 1, in which diffraction peaks tended to shift to the low-angle area due to the enlarged lattice constant by the introduction of larger Dy ions. The change of lattice constant *a* and *c*, that had been normalized by the lattice constant of $Yb_{0.9}Dy_{0.1}MnO_3$, was plotted in Fig. 2. It was noteworthy that cell parameters increase with the rise of Dy content, proving that Dy ions had been doped into the crystal lattice. In addition, we had also found that the alternation of lattice constant *a* was much faster than *c* when Dy content was being increased. Finally, the structure of $DyMnO_3$ turned out to be orthorhombic.[21] In other words, it appeared that the distortion of $YbMnO_3$ structure had been enhanced by doping Dy ions which were slightly larger than Yb ions. When the degree of doping was within the range of x=0.1 to x=0.4, the resulting distortion also changed simultaneously, as demonstrated by the continuous decrease of all peaks. However, in the XRD pattern of sample $Yb_{0.5}Dy_{0.5}MnO_3$, the [002] peak at 16° shifts to the low-angle area, whereas the peaks between 28 and 35° shift to the high-angle area, suggesting that distortion should be different from the one in $Yb_{1-x}Dy_xMnO_3$ ($0.1\leq x\leq 0.4$) samples. This result also indicated that the structure of $Yb_{0.5}Dy_{0.5}MnO_3$ should be hexagonal, even though the change to orthorhombic structure might have been initiated.

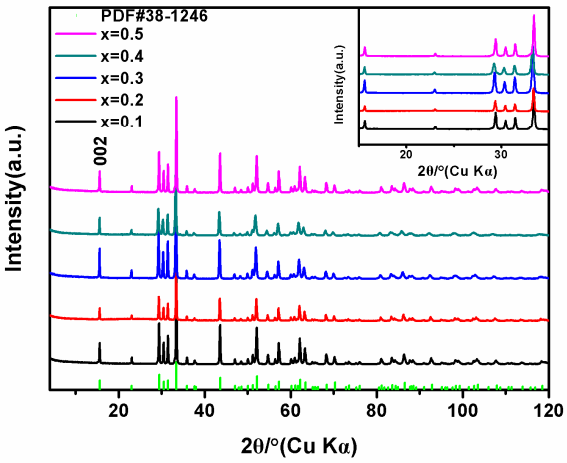

Fig. 1 XRD patterns of *h*-$Yb_{1-x}Dy_xMnO_3$ ($0.1\leq x\leq 0.5$) and the inset shows the part from 15 to 35°

Theoretically, the magnetic properties of $Yb_{1-x}Dy_xMnO_3$ samples are determined by the spins of Yb, Dy and Mn atoms, in which the valence of Yb and Dy is only 3+, whereas the valence of Mn can fluctuate. Consequently, we carried out a series of XPS measurements to understand the exact valence of Mn ions in these compounds. Fig. 3 showed the XPS spectra of $Yb_{1-x}Dy_xMnO_3$ ($0.1\leq x\leq 0.5$) samples, and the binding energy(BE) of Mn $2p_{3/2}$ of $Yb_{1-x}Dy_xMnO_3$ (x=0.1-0.5) was found to be 641.87, 642.04, 642.17, 642.21, 642.24 eV, respectively, consistent with the one observed in

$YbMnO_3$.[22] These results had suggested that Mn ions in the $Yb_{1-x}Dy_xMnO_3$ ($0.1 \le x \le 0.5$) system could only exist as Mn^{3+}, and their BEs seemed to fluctuate with the doping of Dy ions.

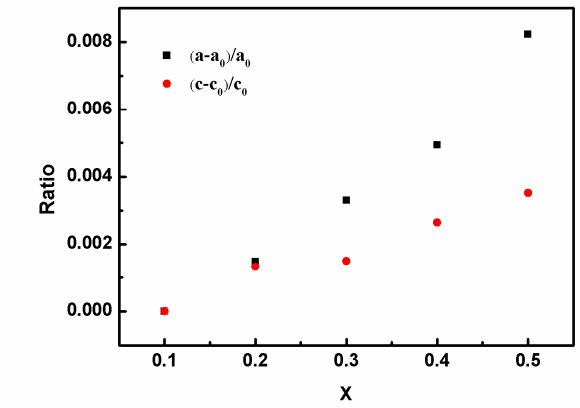

Fig. 2 The rate of absolute changes for lattice constants a and c

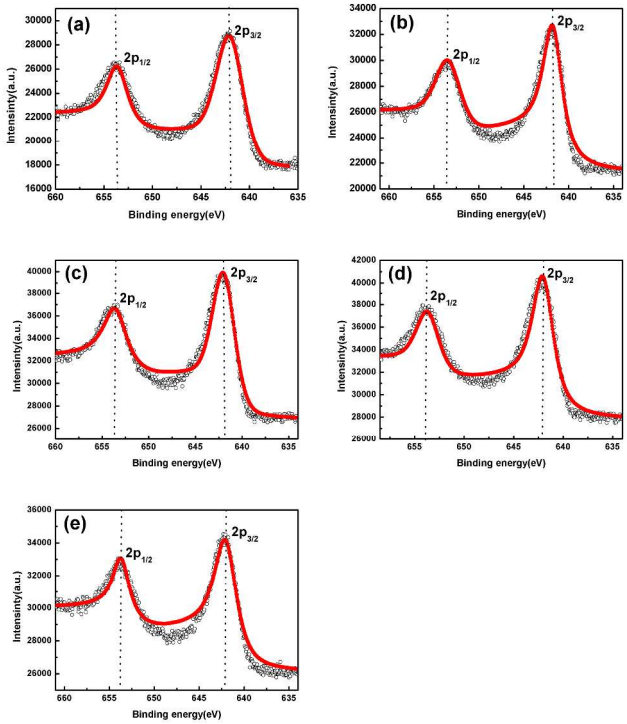

Fig. 3 High-resolution XPS spectra of Mn 2p for $Yb_{1-x}Dy_xMnO_3$: (a)x=0.1, (b)x=0.2, (c)x=0.3, (d)x=0.4, (e)x=0.5

Fig. 4 showed the temperature dependences of magnetization (M-T) for $Yb_{1-x}Dy_xMnO_3$ ($0.1 \le x \le 0.5$) from 2 to 300 K. Obviously, the susceptibility started to increase around 18 K, and a peak around 10K appears when cooling was conducted in the absence of magnetic field. However, it appeared that the susceptibility increased without displaying of peaks below 18K when cooling was carried out under magnetic field of H = 50 Oe. These results indicated that the $Yb_{1-x}Dy_xMnO_3$ ($0.1 \le x \le 0.5$) system should exhibit antiferromagnetic properties but with spin canting ferromagnetism. The Néel temperature was found to be 4.4 K, and no other antiferromagnetic behavior was found at high temperature. Interestingly, results obtained from this work are similar to what Midya reported,[23] whereas different from what Makoto Tachibana disclosed.[24] Presumably, this is because the former used Mn_3O_4 as starting material, which is quite similar to ours, but the later used Mn_2O_3 as the starting materials under high pressure conditions.

Fig. 5 showed the hysteresis loops of $Yb_{1-x}Dy_xMnO_3$ ($0.1 \le x \le 0.5$) samples. Notably, it appeared that the paramagnetic behavior was evident in the loops at 20 K, whereas the ferromagnetic behavior could be seen in the loops at 5 K, proving the presence of canting ferromagnetism as determined by the analysis of M-T curves. When the amount of Dy ions doped was from 0.1 to 0.5, the magnetization susceptibility at 5K under the magnetic field of 3000 Oe was found to be 4.2, 5.2, 6.8, 9, 11 emu/g, respectively. Due to more spins existing in Dy ions, increasing the amount of Dy ions would significantly increase the susceptibilities of $Yb_{1-x}Dy_xMnO_3$ compounds. Because no antiferromagnetic behavior was found at high temperature, the antiferromagnetism and the spin canting ferromagnetism might be due to Yb/Dy ions.

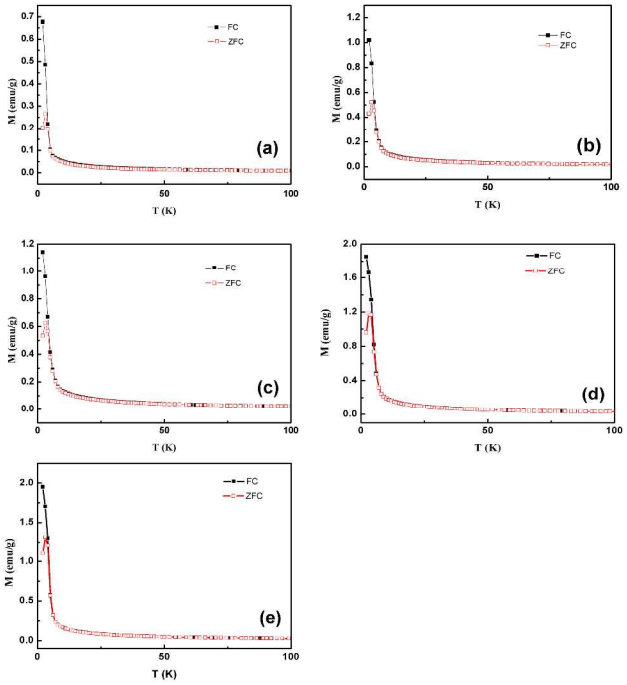

Fig. 4 Temperature dependence of magnetization for $Yb_{1-x}Dy_xMnO_3$: (a)x=0.1, (b)x=0.2, (c)x=0.3, (d)x=0.4, (e)x=0.5

Theoretically, the magnetism of orthorhombic $DyMnO_3$ can be explained by the3D Heisenberg model, whereas the magnetism of hexagonal $YbMnO_3$ can be explained by the chiral 3D Heisenberg model.[25] Upon Dy ions doping, the structure and magnetic property of $YbMnO_3$ will be gradually altered. Accordingly, the distortion occurred within the structure of $Yb_{0.5}Dy_{0.5}MnO_3$ appeared to be very special, which possibly could be located at the boundary between the hexagonal phase and orthorhombic phase. In addition, it was found that high pressure can be an effective tool to modulate the structure of crystals. As a matter of fact, the $Yb_{0.5}Dy_{0.5}MnO_3$ single crystal prepared in this work turned out to be powder-like material. Using KCl as the flux, we were able to synthesize $Yb_{0.5}Dy_{0.5}MnO_3$ single crystal at 1273 K under a 5 GPa pressure.

We next conducted single crystal XRD analysis on suitable $Yb_{0.5}Dy_{0.5}MnO_3$ single crystals with a typical dimension of 0.12 × 0.09 × 0.05 mm. Intensity data were collected at a temperature of 296 K on a Bruker SMART APEX Ⅱ micro-focused diffractometer with graphite-monochromated Mo *Ka* radiation (λ= 0.71073 nm) at 50 kV and 0.6 mA, and then processed with APEX 2 program. Structures were firstly obtained by a direct method and then refined

by full-matrix least-square techniques using SHELXTL crystallographic software package.[26] Notably, heavy atoms, such as Mn, Yb, and Dy, appeared to preside in Fourier maps, and O atoms were also evident in the subsequent difference Fourier maps. The final cycles of least-square refinement included atomic coordinates and anisotropic thermal parameters for all atoms converged at R_1 = 0.0177, wR_2 = 0.0402, and S =1.104. A summary of crystallographic data was presented in Table 1. The selected bond lengths [Å] and angles [deg] were included in Table S1 of the supporting information. Atomic coordinates and equivalent isotropic displacement parameters were also shown in Table S2 of the supporting information.

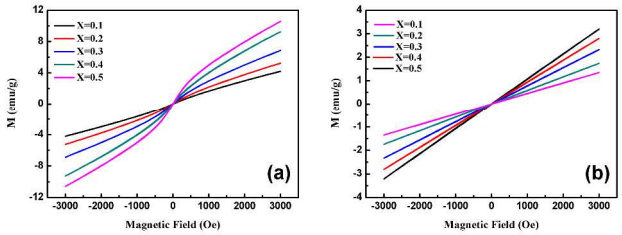

Fig. 5 Magnetic field dependence of the magnetization of $Yb_{1-x}Dy_xMnO_3$ ($0.1 \le x \le 0.5$) at (a) 5K, (b) 20K

Fig. 6 showed the powder XRD patterns of $Yb_{0.5}Dy_{0.5}MnO_3$, and the results were consistent with the simulated XRD patterns based on single-crystal structural analysis of $Yb_{0.5}Dy_{0.5}MnO_3$. Therefore, we concluded that this compound could possess an iso-structure and secondary phase should not be involved. Probably, the intensity difference of certain reflections between the experimental XRD patterns and simulated ones could be the result of preferential orientation.

Table 1 Crystal data and structure refinement for $Yb_{0.5}Dy_{0.5}MnO_3$

Empirical formula	$Yb_{0.5}Dy_{0.5}MnO_3$
Formula weight	270.71
Temperature	293(2) K
Wavelength	0.71073 A
Crystal system, space group	Orthorhombic, *Pnma*
Unit cell dimensions	a = 5.8352(12)Å α=90°
	b = 7.3473(15) Å β = 90°
	c = 5.2561(10) Å γ = 90°
Volume	225.34(8) $Å^3$
Z	4
Theta range for data collection	4.77 —27.09 °
Limiting indices	$-7 \le h \le 6$, $-8 \le k \le 9$, $-6 \le l \le 4$
Reflections collected / unique	4014 / 791 [R(int) = 0.0192]
Completeness to theta = 27.09	100.0 %
Refinement method	Full-matrix least-squares on F^2
Data / restraints / parameters	268 / 0 / 30
Goodness-of-fit on F^2	1.201
Final R indices [I>2sigma(I)]	R_1 = 0.0171, wR_2 = 0.0397
R indices (all data)	R_1 = 0.0177, wR_2 = 0.0402
Largest diff. peak and hole	1.028 and -2.479 $e.Å^{-3}$

Because Dy^{3+} and Yb^{3+} ions have similar scattering factors, their distribution should be uniform in such perovskite structure, therefore, these two sites could be equally processed. Orthorhombic $Yb_{0.5}Dy_{0.5}MnO_3$ crystallizes in the *Pnma* space group, and its crystal structure can be characterized by tilting the ideal MnO_6 octahedral structure of perovskite to afford a distorted hexagonal structure. The bond length of Mn-O(1) and Mn-O(2) was 1.947 and 1.908 Å, respectively; the bond angle of Mn-O(1)-Mn and Mn-O(2)-Mn was 141.3 and 143.4°, respectively. Interestingly, this result was different from what was observed in the hexagonal $Yb_{0.5}Dy_{0.5}MnO_3$ compound.[27]

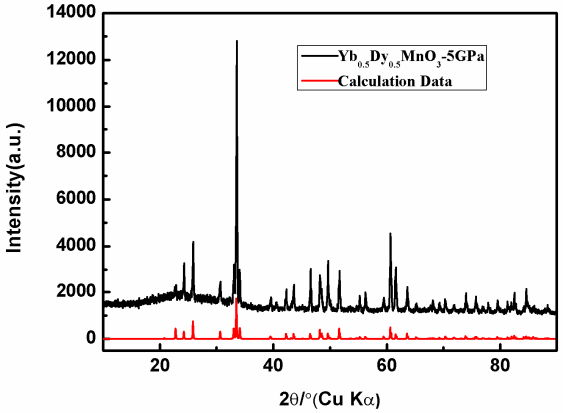

Fig. 6 Experimental XRD pattern and calculated powder XRD pattern of *o*-$Yb_{0.5}Dy_{0.5}MnO_3$

Because valence states can play influential roles on magnetic properties, the valence state of Mn ions had been determined by XPS analysis, and the Mn 2p spectra of *o*-$Yb_{0.5}Dy_{0.5}MnO_3$ manganite were illustrated in Fig. 7. Notably, the $2p_{1/2}$ and $2p_{3/2}$ spectra of Mn displayed broad lines with maxima value of 642.1eV and 653.3eV, respectively, suggesting that the Mn^{3+} ions are the major Mn species present in the single crystal of orthorhombic $Yb_{0.5}Dy_{0.5}MnO_3$.

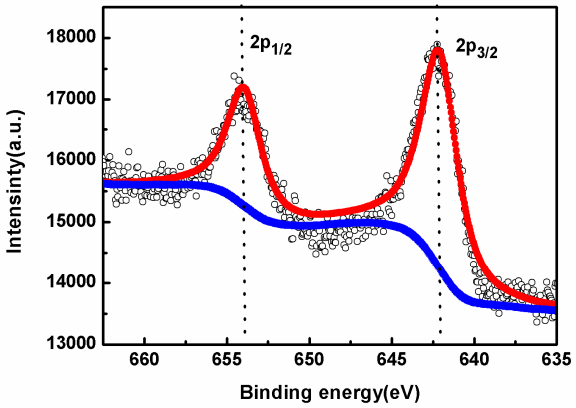

Fig. 7 High-resolution XPS spectrum of Mn 2p for single crystal *o*-$Yb_{0.5}Dy_{0.5}MnO_3$

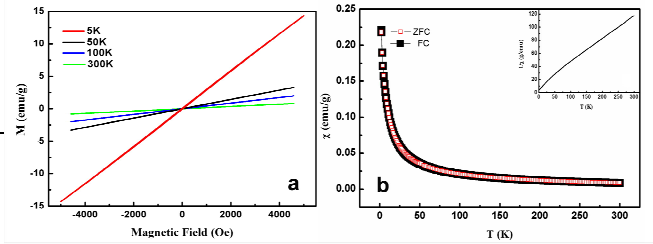

Fig. 8 Field dependence (a) and temperature dependence (b) of magnetization for single crystal *o*-$Yb_{0.5}Dy_{0.5}MnO_3$, the inset of (b) shows the temperature dependence of the inverse magnetic susceptibility of *o*-$Yb_{0.5}Dy_{0.5}MnO_3$

The magnetic susceptibility of $Yb_{0.5}Dy_{0.5}MnO_3$ was measured at a low field of 50 Oe within temperature range of 2-300 K, and the results were shown in Fig. 8. Notably, no antiferromagnetic behaviour was found and typical paramagnetic characteristics were evident, but the reverse of magnetization vs. temperature exhibited little deviation, as shown in the inset of Fig. 8, suggesting that the ferromagnetism in *o*-$Yb_{0.5}Dy_{0.5}MnO_3$ could be very weak. Fig. 8 also included magnetic hysteresis loops measured at 5K, 50 K, 100 K and 300K, respectively. It appeared that these loops were linear, and they did not reach saturation even under a field of 5000 Oe, proving that the antiferromagnetism of *o*-$Yb_{0.5}Dy_{0.5}MnO_3$ might be initiated, but the sample still remained paramagnetic, which meant that the antiferromagnetic order could not exist or its Néel temperature was lower than 2K, our limit of the measurement. Pronounced antiferromagnetism properties were evident in the *h*-$YbMnO_3$ compound, which can be attributed to the triangle magnetism from the hexagonal structure as illustrated by the chiral 3D Heisenberg model. However, it was found that converting *h*-$YbMnO_3$ to *o*-$YbMnO_3$ led to antiferromagnetism, and the magnetic mechanism involved can be explained by typical 3D Heisenberg model. In this work, our results were surprisingly different from the ones reported by others, and we can ascribe the difference among structures. The reported structure of $YbMnO_3$ synthesized under ambient pressure was hexagonal, while the reported $DyMnO_3$ was orthorhombic. The border of the structural transition from hexagonal to orthorhombic is very important to understand the mechanism of the magnetic transition, so we doped the Dy ions into the lattice of $YbMnO_3$ to reach the border. As described above, we found that the structural transition was initiated in the $Yb_{0.5}Dy_{0.5}MnO_3$ powder sample, so we grew the crystal of $Yb_{0.5}Dy_{0.5}MnO_3$ using high-pressure flux method and obtained the *o*-$Yb_{0.5}Dy_{0.5}MnO_3$ crystal, because the reported structure synthesized under high pressure of $YbMnO_3$ was orthorhombic. The T_N of *h*-$YbMnO_3$ was 88 K, and that of *o*-$DyMnO_3$ was 6.5 K, the doping of Dy ions into the lattice of $YbMnO_3$ could lead to the decrease of T_N.[28] The transition of $YbMnO_3$ under high pressure also could lead to the decrease of T_N. Therefore the growth of the crystal of $Yb_{0.5}Dy_{0.5}MnO_3$ under high-pressure might cause the missing of antiferromagnetism due to the slight structural change. Specifically, we discovered that the length of Mn-O(1) bond in the *o*-$Yb_{0.5}Dy_{0.5}MnO_3$ crystal is 1.947 Å, while that of the reported *o*-$YbMnO_3$ and *h*-$YbMnO_3$ is 1.9439 Å and 1.9234 Å, respectively. The bond angle of Mn-O(1)-Mn for the *o*-$Yb_{0.5}Dy_{0.5}MnO_3$ prepared in our laboratory is 141.3°, whereas that of the reported *o*-$YbMnO_3$ and *h*-$YbMnO_3$ is 139.9 and 119.4°, respectively. Consequently, the exchange interaction between Mn atoms was comparatively weaker in the *h*-$Yb_{0.5}Dy_{0.5}MnO_3$ crystal (T_N is 4.4 K), leading to the disappearance of antiferromagnetism. In this work, crystals were re-grown with *h*-$Yb_{0.5}Dy_{0.5}MnO_3$ powder using high-pressure flux method, whereas the reported *o*-$RMnO_3$ compounds were directly synthesized under high pressure in the absence of flux. In addition, this crystal growing process involved the deposition of ions from $Yb_{0.5}Dy_{0.5}MnO_3$ under hydrostatic pressure in liquid environment, but the reported syntheses employed the diffusion of ions from starting materials under quasi-hydrostatic pressure conditions in the presence of inside stress.[24] Consequently, the structure of this crystal would be more stable and uniform when compared with the reported ones,[28] thus its antiferromagnetism could be alleviated or even eliminated. Alternatively, the disappearance of antiferromagnetism could also be due to the increase of average radius of rare earth ions because of Dy doping, which can induce pronounced structural distortion. Overall, this work had endowed a novel *o*-$Yb_{0.5}Dy_{0.5}MnO_3$ crystal featuring decent paramagnetic properties and unique structural distortion.

Conclusions

In summary, a series of hexagonal $Yb_{1-x}Dy_xMnO_3$ ($0.1 \le x \le 0.5$) manganites have been prepared by the traditional solid-state reaction method in order to lower the Néel temperature, and the orthorhombic $Yb_{0.5}Dy_{0.5}MnO_3$ single crystal has been firstly synthesized by a high-pressure flux method because the application of high pressure could lower the Néel temperature. Their magnetism was investigated, subsequent magnetic measurements show that such hexagonal compounds exhibit antiferromagnetic properties with a Néel temperature of 4.4 K, which is lower than the reported temperature, plus, canted antiferromagnetic behaviour has been also observed at lower temperature, which might be due to Yb/Dy ions; Moreover, it appears that the magnetization increases with the rise of Dy dopant content. It is noteworthy that the orthorhombic compound $Yb_{0.5}Dy_{0.5}MnO_3$ has exhibited pronounced paramagnetic properties, differing from the antiferromagnetic $RMnO_3$ compounds reported in the literature, which could be due to the structural difference between them. The disappearance of antiferromagnetism may be beneficial to understanding the mechanism of rare earth manganites.

Acknowledgements

We greatly acknowledge financial support from the National Natural Science Foundation of China (21371068, 20471022 and 40673051).

Notes and references

[a] State Key Laboratory of Inorganic Synthesis and Preparative Chemistry, College of Chemistry, Jilin University, 2699 Qianjin Street, Changchun 130012, P. R. China.
To whom correspondence should be addressed.
E-mail: liuxy@jlu.edu.cn (Xiaoyang Liu)
xdzhao@jlu.edu.cn (Xudong Zhao)
Fax: (+86) 431-85168316
Tel: (+86) 431-85168316

†Electronic Supplementary Information (ESI) available: Bond lengths [Å] and angles [deg] for $Yb_{0.5}Dy_{0.5}MnO_3$ (Table S1); Atomic coordinates and equivalent isotropic displacement parameters ($Å^2$) for $Yb_{0.5}Dy_{0.5}MnO_3$ (Table S2). See DOI: 10.1039/b000000x/

1 Khomskii D. I, *J. Magn. Magn., Mater.* 2006, **306**, 1-8.
2 Shintaro Ishiwata, Yusuke Tokunaga, Yasujiro Taguchi, Yoshinori Tokura, *J. Am. Chem. Soc.,* 2011, **133**,13818-13820.
3 Wang J, Neaton J. B, Zheng H, Nagarajan V, Ogale S. B, Liu B, Viehland D, Vaithyanathan V, Schlom D. G, Waghmare U. V, Spaldin N. A, Rabe K. M, Wuttig M, Ramesh R, *Science*., 2003, **299**, 1719-1722.
4 Azuma M, Takata K, Saito T, Ishiwata S, Shimakawa Y, Takano M, *J. Am. Chem. Soc.,* 2005, **127**, 8889-8892.
5 M. Mostovoy, *Phys. Rev. Lett.,* 2006, **96**, 067601-4.
6 M. Kenzelmann, A. B. Harris, S. Jonas, C. Broholm, J. Schefer, S. B. Kim, C. L. Zhang, S. W. Cheong, O. P. Vajk, J. W. Lynn, *Phys. Rev. Lett.*, 2005, **95**, 087206-4.
7 Zhang J, Xu Y, Cao S, Cao G, Zhang Y, Jing, C, *Phys. Rev. B.,* 2005, **72**, 054410-6.
8 J. S. Zhou, J. B. Goodenough, J. M. Gallardo-Amores, E. Morán, M. A. Alario-Franco, R. Caudillo, *Phys. Rev. B.,* 2006, **74**, 014422-7.
9 Rubi D, Venkatesan Sriram, Kooi B. J, Noheda B, *Phys. Rev. B.,* 2008, **78**, 020408-4.
10 Graboy IE, Bosak AA, Gorbenko OY, Kaul AR, Dubourdieu C, Senateur JP, Svetchnikov VL, Zandbergen HW, *Chem. Mater.,* 2003, **15**, 2632-2637.
11 Fuyang Liu, Junjia Li, Qiliang Li, Ying Wang, Xudong Zhao, Yingjie Hua, Chongtai Wang, Xiaoyang Liu. *Dalton. Trans.,* 2014, **43**, 1691-1698.

12 Monica Esperanza Bolıvar Guarin, Alexandre de Melo Moreira, Nivaldo Lucio Speziali, *J. Appl. Cryst.,* 2013, **46**, 644-648.
13 Koichi Yamada, Toshihiro Okamoto, Kenichi Kudoh, Atsushi Wakamiya, Shigehiro Yamaguchi, J. Takeya, *Appl. Phys. Lett.*, 2007, **90**, 072102-3.
14 Shirakawa Naoki, Ikeda Shin-ichi, Iwasaki Ryusuke, *Appl. Phys. Lett.*, 2005, **87**, 024105-3.
15Youting Song, Wenjun Wang, Wenxia Yuan, Xing Wu, Xiaolong Chen,*J. Crys.Growth,*2003,**247**,275-278.
16 L. I. Hung, S. Wang, S. P. Szu, C. Y. Hsieh, H. M. Kao, K. H. Lii, *Chem. Mater.,* 2004, **16**, 1660-1666.
17 X. G. Zhao, J. Y. Li, P. Chen, Y. Li, Q. X. Chu, X. Y. Liu, J. H. Yu, R. R. Xu, *Inorg. Chem.,* 2010, **49**, 9833-9840.
18 C. S. Chen, S. F. Lee, K. H. Lii, *J. Am. Chem. Soc.,* 2005, **127**, 12208-12209.
19 H. K. Liu, K. H. Lii, *Inorg. Chem.,* 2011, **50**, 5870-5872.
20 T. Katsufuji, S. Mori, M. Masaki, Y. Moritomo, N. Yamamoto, H. Takagi, *Phys. Rev. B.,* 2001, **64**, 104419-6.
21 S Harikrishnan, S Rößler, C M Naveen Kumar, H L Bhat, U K Rößler,S Wirth, F Steglich, Suja Elizabeth, *J. Phys.: Condens. Matter.,* 2009, **21**, 096002-10.
22 T. Kimura, T. Takenaka, S. Fujitsu, K. Shinozaki, *Key Eng. Mater.,* 2003, **248**, 77-82.
23 A. Midya, S. N. Das, P. Mandal, *Phys. Rev. B.,* 2011, **84**, 235127-10.
24 Makoto Tachibana, Tomotaka Shimoyama, Hitoshi Kawaji, Tooru Atake, Eiji Takayama-Muromachi, *Phys. Rev. B.,* 2007, **75**, 144425-5.
25 A. Oleaga, A. Salazar, D. Prabhakaran, J. G. Cheng, J. S. Zhou, *Phys. Rev. B.,* 2012, **85**, 184425.
26 G. M. Sheldrick, SHELXTL Programs, Version 5.1, Bruker AXS GmbH, Karlsruhe, Germany, 1998.
27 Mori T, Aoki K, Kamegashira N, Shishido T, Fukuda T, *Mater. Lett.,* 2000, **42**, 387-389.
28 Y. H. Huang, H. Fjellvåg, M. Karppinen, B. C. Hauback, H. Yamauchi, J. B. Goodenough, *Chem. Mater.,* 2006, **18**, 2130-2134.

